PHYSICAL REVIEW A VOLUME 1, NUMBER 1 JANUARY 1970

Microscopic Theory of Quantum Fluids. I. Quantum Statistical Development

F. Mohling
Department of Physics and Astrophysics, University of Colorado, Boulder, Colorado 80302

I. RamaRao*
Department of Physics, Stanford University, Stanford, California 94305

Dion W. J. Shea†
Aeronomy Laboratory, Environmental Science Services Administration, Boulder, Colorado 80302
(Received 16 June 1969)

A simplified derivation of the master-graph formulation of the quantum-statistical theory of an interacting quantum fluid is presented. A complete analysis of the self-energy structures arising from both particle statistics and particle interactions simplifies the master-graph expressions for the thermodynamic properties of the fluid. The x-ensemble formulation of Lee and Yang is used to treat the degenerate Bose fluid below its Bose-Einstein condensation temperature. The results for a Bose fluid above its Bose-Einstein condensation temperature and for a Fermi fluid are obtained as special cases.

1. INTRODUCTION

The microscopic theory of the low-temperature many-body problem has been approached in recent years by a number of significantly different methods. These methods have included quantum-statistical methods,[1-12] perturbation theory methods,[13-23] and Green's-function techniques.[24-31]

In this paper, we present a unified quantum-statistical theory of equilibrium quantum fluids which is both simple and capable of direct application to the calculation of the macroscopic properties of realistic systems in terms of their fundamental interparticle interactions. The unique feature of the present theory is that it satisfies the following important requirements on any microscopic theory of quantum fluids, namely, (a) the theory applies to finite temperatures as well as to the zero-temperature limit; (b) the theory treats the case of strong interactions so that the repulsive cores of real particles can be included; and (c) the theory obtains a quasiparticle description of the quantum fluid as the result of a thorough and rigorous treatment of the self-energy problem.

It is also worthwhile to indicate at the outset what has not yet been accomplished by the present theory. It has not yet been extended to include the description of transport processes or other nonequilibrium phenomena. It is restricted to single-component quantum fluids, although the generalization to a multicomponent quantum fluid[7] is straightforward. The possibility of describing the phase transition between the liquid and gaseous states of a quantum fluid has not yet been investigated. However, the case of Bose-Einstein condensation, in which macroscopic occupation of a single (one-particle) quantum state occurs in a Bose fluid, is treated.

The unified quantum-statistical theory of low-temperature, equilibrium quantum fluids presented in this paper has been developed over the past several years by one of the authors (F. M.). The primary objective of this development has been to derive useful expressions for the grand potential, from which all the thermodynamic properties of the system can be obtained, and for the various distribution functions, such as the momentum distribution and the pair-correlation function. This development was divided into two parts: (a) the analysis[1,2] of a Bose fluid above its transition temperature or of a Fermi fluid (both referred to here as a "normal" fluid), and (b) the analysis[3,4] of a Bose fluid below its transition temperature (referred to here as a "degenerate" fluid). In a degenerate fluid the macroscopic occupation of a single one-particle quantum state (i.e., the occurrence of Bose-Einstein condensation) requires that the degenerate fluid receive a different treatment from the normal fluid. The purpose of the present paper is to extend, synthesize, and simplify the previous analyses of quantum fluids and to include the normal fluid as a special case of the degenerate fluid.

Before considering the new developments let us first review the previous analyses of quantum fluids. The Ursell expansion was used[1,3] to express the grand potential and the distribution functions in terms of cluster integrals. As a first step in studying the cluster integrals, a partial summa-

tion in the theory was performed to express the cluster integrals in terms of the free-particle momentum distribution

$$\nu(k) = \exp\beta[g - \omega(k)]\{1 - \epsilon \exp\beta[g - \omega(k)]\}^{-1} \quad , \quad (1.1)$$

instead of in terms of the basic statistical factor $\epsilon \exp\beta[g - \omega(k)]$. Here, we have $\epsilon = +1$ for a Bose fluid, and $\epsilon = -1$ for a Fermi fluid. Furthermore, the effects of particle interactions were accounted for by performing a linked-pair expansion in which the cluster integrals were expressed in terms of two-body functions related to the matrix elements of the interaction potential. The theory was then expanded in terms of linked-pair graphs in which the effects of particle statistics were related to solid lines and the effects of particle interactions were related to wiggly lines.

In order to express the theory in terms of quantities that are more physical than the free-particle momentum distribution, the next step in the development was to analyze the self-energy problem (i.e., to study all graphical structures with one or two external lines). The self-energy analysis[2,3] was divided into the study of three types of graphs: those with just solid external lines (statistical effects); those with just wiggly external lines (dynamical – or interaction – effects); and those with both solid and wiggly external lines (mixing the effects of statistics and dynamics). After this complicated self-energy analysis, the theory was reexpressed in terms of master graphs in which the line factors represented all of the possible contributions from self-energy graphs. These line factors were obtained as solutions of a complicated set of coupled integral equations.

Finally, a partial solution of these integral equations gave the dominant low-temperature contributions to the line factors, and the Λ transformation was applied to the theory to account consistently for the corrections to these dominant low-temperature contributions.[2,4] The Λ transformation resulted in a quasiparticle description of the system. This entire analysis was an extension of earlier work by Lee and Yang.[8–10]

Recently, we have found that the set of coupled integral equations for the self-energy contributions can be considerably simplified if the effects of mixing statistics and dynamics are fully utilized. This new analysis results in simpler expressions for the master-graph expansions of the grand potential and the momentum distribution, and simplifies calculations. Although we can derive this new formulation from the previous results, we have also obtained a deeper insight into the self-energy problem, which indicates that much of the previous complicated analysis can be eliminated.

In reexamining our previous analysis of quantum fluids, we find that two "unfortunate" steps were taken: The first was the partial summation of the theory in which the basic statistical factor $\epsilon \exp\beta[g - \omega(k)]$ was replaced by the free-particle momentum distribution $\nu(k)$. {Since much of the earlier self-energy analysis was devoted to the replacement of $\nu(k)$ by a more physically meaningful quantity, one closely related to the actual momentum distribution for an interacting system, it is simpler to work directly with the basic statistical factor $\epsilon \exp\beta[g - \omega(k)]$ without ever introducing $\nu(k)$.} The second "unfortunate" step was to keep separate the effects of statistics and dynamics until the master graphs were introduced, when the mixing of these two effects was finally considered. By mixing the effects of statistics and dynamics from the outset, we find now that the self-energy problem can be analyzed in a clearer and more illuminating manner. To summarize, two important steps in the previous analysis are eliminated, resulting in a considerable simplification of the entire analysis. In making these changes we depart almost entirely from the original viewpoint of Lee and Yang[8–10] which formed the basis of the previous analysis.

In Sec. 2, we use the linked-pair expansion to express the theory in terms of primary linked-pair graphs. In Sec. 3, we analyze the zero-momentum self-energy graphs (for a degenerate fluid). In Sec. 4, we analyze the nonzero-momentum self-energy graphs and express the momentum distribution in terms of master graphs. In Sec. 5, we express the grand potential in terms of master graphs.

2. REVIEW OF QUANTUM STATISTICS

The theory of the grand canonical ensemble provides a means of calculating average values and fluctuations of the energy, total number of particles, entropy, and other equilibrium thermodynamic properties, as well as the distribution functions, for a system of interacting particles. The calculation of the average values of the thermodynamic properties of a system essentially reduces to the determination of the grand partition function:

$$\exp(\Omega f) = \sum_{N=0}^{\infty} \mathrm{Tr}_N[\exp(\beta g N)\exp(-\beta H^{(N)})] \quad , \quad (2.1)$$

where Ω is the volume, f is the grand potential (assumed to be an intensive quantity), g is the chemical potential, N is the number operator, $\beta = 1/\kappa T$, κ is Boltzmann's constant, and T is the absolute temperature. We make the usual assumption that the N-particle Hamiltonian $H^{(N)}$ includes only two-body interactions, although this assumption is not essential to the method. The symbol Tr_N indicates that the trace is to be taken over a complete set of properly symmetrized (or antisymmetrized) N-particle state vectors. If we use the interaction picture and express the N-particle state vectors as symmetrized (or antisymmetrized) combinations of single-particle state vectors in the momentum representation, the Tr_N term in Eq. (2.1) takes the form

$$\mathrm{Tr}_N[\exp(\beta g N)\exp(-\beta H^{(N)})] = (N!)^{-1} \sum_{k_1 \cdots k_N} \exp\Big(\beta \sum_{i=1}^{N} [g - \omega(k_i)]\Big)$$

$$\times \sum_{P'} \epsilon^{P'} \langle k_1 k_2 \cdots k_N | W_N(\beta) | k_1' k_2' \cdots k_N' \rangle \big|_{k_i' = k_i} , \tag{2.2}$$

where $$W_N(\beta) \equiv \exp(\beta H_0^{(N)}) \exp(-\beta H^{(N)}) ; \tag{2.3}$$

$H_0^{(N)}$ is the free N-particle Hamiltonian; $\omega(k) = \hbar^2 k^2/2M$; $\epsilon = +1$ for Bose-Einstein statistics, and $\epsilon = -1$ for Fermi-Dirac statistics; and $\sum_{P'} P'$ indicates the sum over all possible permutations of the primed indices. We use the convention that k represents all the eigenvalues necessary to specify a single-particle state of $H_0^{(1)}$.

For a degenerate Bose fluid, Lee and Yang[9] found that the usual methods for determining the grand potential failed because of the macroscopic occupation of the zero-momentum single-particle state. If L of the single-particle states used in the trace in Eq. (2.1) correspond to zero-momentum states, then there are $L!$ identical exchange terms in the matrix elements contributing to this trace [see Eq. (2.2)]. This very large number of exchange terms, for $\langle L \rangle \sim \langle N \rangle$, results in a nonintensive expression for the grand potential which diverges as $\Omega \to \infty$.

To overcome this problem, Lee and Yang[10] suggested using a modification of the grand canonical ensemble that they called the x ensemble. In the x ensemble, Eq. (2.1) is replaced by

$$\exp(\Omega f_x) = \exp(-x\Omega) \sum_{N=0}^{\infty} \sum_{L=0}^{N} \frac{(x\Omega)^L}{L!} \mathrm{Tr}_{N,L}[\exp(\beta g N)\exp(-\beta H^{(N)})] , \tag{2.4}$$

where the symbol $\mathrm{Tr}_{N,L}$ indicates that the trace is to be taken over a complete set of N-particle states in the momentum representation in which L of the free, single-particle states have zero-momentum. The parameter x is determined from the theorem that if

$$\partial f_x / \partial x = 0, \quad \text{at} \quad x = \langle x \rangle = \Omega^{-1} \langle L \rangle , \tag{2.5}$$

then $f_x = f$ in the limit $\Omega \to \infty$. If Eq. (2.5) is not satisfied, then $f_x = f$ at $\langle x \rangle = 0$, and Eq. (2.4) reduces essentially to Eq. (2.1). From Eq. (2.5) we see that the parameter x is the density of zero-momentum particles and that f_x is equal to the grand potential f at equilibrium. Some of the implications of Eqs. (2.4) and (2.5) are discussed in Ref. 3 [below Eq. (3) in that reference].

If we develop the quantum-statistical theory using the x-ensemble, and allow the N-particle state vectors used in evaluating the traces in Eq. (2.4) to be either symmetrized or antisymmetrized as in Eq. (2.2), we see that we can simultaneously treat the cases of a Bose fluid below the Bose-Einstein condensation temperature ($\epsilon = +1$, $\langle x \rangle > 0$), a Bose fluid above the Bose-Einstein condensation temperature ($\epsilon = +1$, $\langle x \rangle = 0$), and a normal Fermi fluid ($\epsilon = -1$, $\langle x \rangle = 0$). In the latter two cases (the normal fluid), we set $\langle x \rangle = 0$ [which is equivalent to setting all the (0, 2) and (2, 0) quantities that we shall introduce later equal to zero] and *include $k = 0$ in all of the momentum state sums.*

We begin our analysis with the expressions found previously for the grand potential and the momentum distribution in terms of linked-pair (μ, ν) graphs. The grand potential is given by

$$\Omega f(x, \beta, g, \Omega) = \Omega f_0(\beta, g, \Omega) - x\Omega + x\Omega e^{\beta g} + \sum [\text{all different linked-pair (0, 0) graphs}] , \tag{2.6}$$

where the free-particle grand potential is

$$\Omega f_0(\beta, g, \Omega) = -\epsilon \sum_p \ln\{1 - \epsilon \exp\beta[g - \omega(p)]\} \ , \tag{2.7}$$

and the momentum distribution is given by

$$\langle n(k)\rangle = \langle x\rangle \Omega \delta_{k,0} + \nu(p)[1 + \epsilon\nu(p)] \sum[\text{all different linked-pair } (1,1) \text{ graphs}]_p, \tag{2.8}$$

where the free-particle momentum distribution is

$$\nu(p) = \exp\beta[g - \omega(p)]\{1 - \epsilon \exp\beta[g - \omega(p)]^{-1}\} \ . \tag{2.9}$$

Equations (2.6) and (2.7) follow from Eqs. (16) and (17) in Ref. 3 and Eqs. (57) and (22) in Ref. 1, while Eq. (2.8) follows from Eqs. (27) and (29) in Ref. 3 and Eqs. (9) in Ref. 2. We use the convention (when $\langle x\rangle \neq 0$) that whenever a momentum k *does not* take the value zero it is represented by p.

The definition of linked-pair (μ, ν) graphs, which are similar to the primary linked-pair (μ, ν) graphs we shall introduce below, can be determined from Refs. 1 and 3. Among other things, linked-pair (μ, ν) graphs contain solid lines with line factors $\epsilon\nu(p)$, where $\nu(p)$ is the free-particle momentum distribution, and cluster vertex functions[32]

$$\begin{aligned} {}^{t_1 t_2}\begin{bmatrix} k_1 k_2 \\ k_3 k_4 \end{bmatrix}_{t_0} \exp\{-t_0[\omega(k_1) + \omega(k_2) - \omega(k_3) - \omega(k_4)]\} &\equiv \theta(t_1 - t_2)\, {}^{t_2}\begin{bmatrix} k_1 k_2 \\ k_3 k_4 \end{bmatrix}_{t_0} \theta(t_2 - t_0) + \theta(t_2 - t_1)\, {}^{t_1}\begin{bmatrix} k_1 k_2 \\ k_3 k_4 \end{bmatrix}_{t_0} \theta(t_1 - t_0), \\ &\qquad \text{for } t_1 \neq t_2 \ , \\ &= {}^{t_1}\begin{bmatrix} k_1 k_2 \\ k_3 k_4 \end{bmatrix}_{t_0} \theta(t_1 - t_0), \quad \text{for } t_1 = t_2, \end{aligned} \tag{2.10}$$

where $\theta(y) = 0$ for $y < 0$, $\theta(y) = 1$ for $y > 0$, and

$$\begin{aligned} {}^{t_1}\begin{bmatrix} k_1 k_2 \\ k_3 k_4 \end{bmatrix}_{t_0} &\equiv \{\langle k_1 k_2 \mid R(t_1, t_0) \mid k_3 k_4\rangle + \epsilon\langle k_1 k_2 \mid R(t_1, t_0) \mid k_4 k_3\rangle\} \exp\{-t_0[\omega(k_1) + \omega(k_2) - \omega(k_3) - \omega(k_4)]\} \ , \\ R(t_1, t_0) &\equiv -\frac{\partial}{\partial t_0}\{\exp[t_1 H_0^{(2)}] \exp[-(t_1 - t_0)H^{(2)}] \exp[-t_0 H_0^{(2)}]\} \ . \end{aligned} \tag{2.11}$$

The $\epsilon\nu(p)$ arise by summing [for every internal line in the corresponding linked-pair (μ, ν) graph] all possible numbers of one-body functions, each of which represents the basic statistical factor $\epsilon \exp\beta[g - \omega(p)]$. Unfortunately, the free-particle momentum distribution is not a useful function for an interacting system. The entire statistical analysis is simplified if instead we use primary linked-pair (μ, ν) graphs, which are expressed in terms of the basic statistical factor $\epsilon \exp\beta[g - \omega(p)]$ rather than $\epsilon\nu(p)$. We now define primary linked-pair (μ, ν) graphs.

Primary Linked-Pair $(\mu\nu)$ Graphs

A primary linked-pair (μ, ν) graph is a collection of P cluster vertices and P_1 1-vertices. The expressions represented by these two types of vertices are shown in Fig. 1. These vertices are entirely interconnected by m wiggly (internal) lines. There are also m_{do} outgoing dotted lines and m_{di} incoming dotted lines, and we shall also refer to these dotted lines as being internal lines. The expressions represented by these lines are shown in Fig. 2. In addition to internal lines, there are μ outgoing external solid lines and ν incoming external solid lines. Some examples of primary linked-pair (μ, ν) graphs are given in Fig. 3. The rules for forming these graphs and the procedure for determining the expression corresponding to a given graph are as follows:

(a) A 1-vertex is represented by a cross and has attached one outgoing and one incoming line, neither of which may be a dotted line. A cluster vertex is represented by a circled dot and has attached two outgoing and two incoming lines which may be solid, wiggly, or dotted. It must not be possible to complete a loop in a primary linked-pair (μ, ν) graph by following the arrows on wiggly lines without encountering at least one 1-vertex. Two wiggly lines may not connect the same two cluster vertices; such a structure is called a wiggly-line double bond.

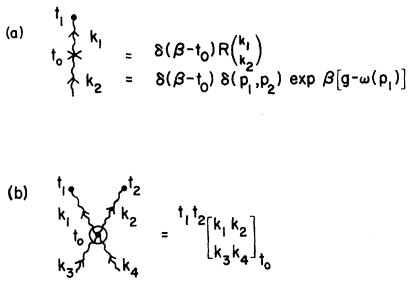

FIG. 1. Expressions represented by 1 vertices and cluster vertices. Both types of vertices occur in primary linked-pair and zero-contracted (μ, ν) graphs, while only cluster vertices appear in master (μ, ν) graphs. When k cannot be zero, we make the replacement $k \to p$. The lines which attach to cluster vertices can also be dotted. (a) 1 vertex. (b) Cluster vertex.

(b) To each external (solid) line assign a pregiven momentum p. External lines with different assigned momenta are considered distinguishable. For the case $\langle x \rangle \neq 0$, when an external momentum is zero, there is no corresponding external line. For the purpose of rule (e), associate a temperature label β with each outgoing solid line.

(c) Two primary linked-pair (μ, ν) graphs are different if their topological structure, including internal line types and directions, and external line momenta and direction are different.

(d) To each internal wiggly line assign a different integer $i (i = 1, 2, \ldots, m)$ and a momentum k_i. To each outgoing dotted line assign a different integer $i (i = m+1, m+2, \ldots, m+m_{do})$, a zero momentum, a temperature label s_i, and an outgoing zero-momentum line factor $\delta(\beta - s_i)(x\Omega)^{1/2} \exp\beta g$. To each incoming dotted line assign a different integer $i (i = m+m_{do}+1, \ldots, m+m_{do}+m_{di})$, a zero-momentum, and an incoming zero-momentum line factor $(x\Omega)^{1/2}$.

(e) Assign a temperature label t_j to each 1-vertex and each cluster vertex. Associate a vertex function with each vertex as shown in Fig. 1. Momentum is conserved at each vertex. Graphical structures in which some of the wiggly-line momenta are identically zero must also be included in any sum over all primary linked-pair (μ, ν) graphs.

(f) Form a product of all the line factors and vertex functions assigned in rules (d) and (e). Assign an over-all sign ϵ^{P_B} to the entire graph, where P_B is the permutation of the $(2P + P_1)$ bottom-row momenta of the vertex functions with respect to the $(2P + P_1)$ top-row momenta.

(g) Assign a factor S^{-1} to the entire graph, where $S \equiv$ symmetry number .

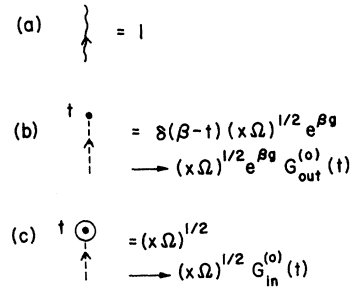

FIG. 2. Expressions represented by lines in primary linked-pair and zero-contracted (μ, ν) graphs. (a) A wiggly line. (b) An outgoing dotted (zero-momentum) line. The first expression is for a primary linked-pair (μ, ν) graph, and the second expression is for a zero-contracted (μ, ν) graph. (c) An incoming dotted (zero-momentum) line. The first expression is for a primary linked-pair (μ, ν) graph, and the second expression is for a zero-contracted (μ, ν) graph. Here, the temperature label t is that of the cluster vertex to which the incoming dotted line attaches.

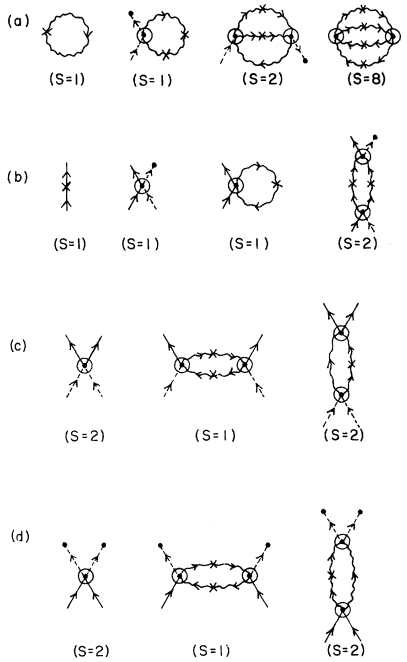

FIG. 3. Some examples of primary linked-pair (a) (0, 0) graphs, (b) (1, 1) graphs, (c) (2, 0) graphs, and (d) (0, 2) graphs. The symmetry number of each graph is shown.

The symmetry number is defined to be the total number of permutations of the $(m+m_{do}+m_{di})$ integers assigned to the internal lines that leave the graph topologically unchanged (including the positions of these numbers relative to the internal lines). Examples of symmetry numbers are given in Fig. 3.

(h) Finally, sum over all of the m nonzero, internal momenta and integrate each of the $(P+P_1+m_{do})$ temperature variables from 0 to β.

It is also necessary to give a general definition of *a* (μ,ν) *L graph*. Corresponding to any given type of (μ,ν) graph $(\mu,\nu)\neq(0,0)$, we can define a (μ,ν) L graph which has the same structure and rules as the corresponding (μ,ν) graph with the following exceptions:

(i) The external lines are represented by wiggly lines assigned pregiven momenta $k(=0$ or $p)$.

(ii) A temperature label $t(t\leq\beta)$ is assigned to the head end of each outgoing external wiggly line (if any).

(iii) The temperature label of any vertex to which an incoming external wiggly line (if any) attaches is not integrated over.

The concept of a (μ,ν) L graph applies to the zero-contracted, master, and transformed master (μ,ν) graphs which will be introduced later, as well as to primary linked-pair (μ,ν) graphs.

In terms of primary linked-pair (μ,ν) graphs, the grand potential is given by

$$\Omega f(x,\beta,g,\Omega)=(x\Omega)\exp\beta g-(x\Omega)+\sum[\text{all different primary linked-pair (0, 0) graphs}], \tag{2.12}$$

and the momentum distribution is given by

$$\langle n(k)\rangle=\langle x\rangle\Omega\delta_{k,0}+\exp\beta[g-\omega(p)]\{1+\epsilon\sum[\text{all different primary linked-pair (1, 1) graphs}]_p\}\ . \tag{2.13}$$

We could obtain Eqs. (2.6) and (2.8) from Eqs. (2.12) and (2.13), respectively, by integrating over the temperature labels associated with the 1-vertices in the primary linked-pair (μ,ν) graphs and then [for every internal line in the corresponding linked-pair (μ,ν) graph] summing over all possible numbers of 1-vertices to obtain linked-pair (μ,ν) graphs.

3. ZERO-MOMENTUM SELF-ENERGY STRUCTURES

We begin our analysis of self-energy structures by considering zero-momentum self-energy structures. By a zero-momentum self-energy structure we mean a graphical structure with only one "external" line that could attach to a cluster vertex. In primary linked-pair (μ,ν) graphs there occur graphs in which conservation of momentum at the vertices requires that some of the wiggly lines have momenta that are identically zero $(k\equiv 0)$. For such graphs, we can separate the graphs into two disconnected parts by cutting one of these $k\equiv 0$ wiggly lines. We shall perform a partial summation of the primary linked-pair (μ,ν) graphs in which these $k\equiv 0$ wiggly lines are eliminated, and their effects are accounted for by generalizing the line factors associated with the zero-momentum dotted lines. We note that the analysis of this section applies, of course, only to a Bose fluid below its transition temperature and is essentially the same as the analysis given in Sec. 5 of Ref. 3.

A (μ,ν) graph is *improper with respect to* $k\equiv 0$ *wiggly lines* if by cutting any one of its $k\equiv 0$ wiggly lines the graph can be separated into two disconnected graphs. A *proper* (μ,ν) *graph with respect to* $k\equiv 0$ *wiggly lines* is a (μ,ν) graph which is not improper with respect to such lines. Thus, a (μ,ν) graph is improper (proper) with respect to $k\equiv 0$ wiggly lines if it contains (does not contain) $k\equiv 0$ wiggly lines.

In order to perform the partial summation over $k\equiv 0$ wiggly lines in primary linked-pair (μ,ν) graphs we introduce *zero-contracted* (μ,ν) *graphs*. The rules for forming zero-contracted (μ,ν) graphs and determining the corresponding expressions are the same as for primary linked-pair (μ,ν) graphs with the following changes:

(a) A zero-contracted (μ,ν) graph is proper with respect to $k\equiv 0$ wiggly lines, i.e., it does not contain any $k\equiv 0$ wiggly lines.

(b) The line factor for an outgoing dotted (zero-momentum) line is $(x\Omega)^{1/2}e^{\beta g}G_{\text{out}}^{(0)}(t)$ and the line factor for an incoming dotted (zero-momentum) line is $(x\Omega)^{1/2}G_{\text{in}}^{(0)}(t)$, where

$$G_{\text{out}}^{(0)}(t)\equiv\delta(\beta-t)+K_{\text{out}}^{(0)}(t)\ ,$$

$$G_{\text{in}}^{(0)}(t)\equiv 1+K_{\text{in}}^{(0)}(t)\ . \tag{3.1}$$

In $G_{\text{in}}^{(0)}(t)$, t is the temperature label of the cluster vertex to which the incoming dotted line attaches.

Consider a cluster vertex in a zero-contracted (μ,ν) graph to which a dotted line is attached. It should be

clear that, in terms of primary linked-pair (μ, ν) graphs, the $\delta(\beta - t)$ term in $G_{\text{out}}^{(0)}(t)$ represents an outgoing dotted line, while $K_{\text{out}}^{(0)}(t)$ represents the sum over all possible graphical structures which can attach to the cluster vertex with an outgoing $k \equiv 0$ wiggly line. Similarly the "1" term in $G_{\text{in}}^{(0)}(t)$ represents an incoming dotted line, while $K_{\text{in}}^{(0)}(t)$ represents the sum over all possible graphical structures which can attach to the cluster vertex with an incoming $k \equiv 0$ wiggly line. The quantities $K_{\text{out}}^{(0)}(t)$ and $K_{\text{in}}^{(0)}(t)$ can be defined by functional derivatives as

$$K_{\text{out}}^{(0)}(t) = (x\Omega e^{\beta g})^{-1}[\delta/\delta G_{\text{in}}^{(0)}(t)]\sum[\text{all different zero-contracted } (0,0) \text{ graphs}] \ , \tag{3.2}$$

$$\text{and } K_{\text{in}}^{(0)}(t) = (x\Omega e^{\beta g})^{-1}[\delta/\delta G_{\text{out}}^{(0)}(t)]\sum[\text{all different zero-contracted } (0,0) \text{ graphs}] \ . \tag{3.3}$$

In each of these derivatives, the vertex functions are held constant, and one of the temperature integrations in the zero-contracted (0, 0) graph is eliminated. In Eq. (3.2) we obtain $(x\Omega)^{1/2}e^{\beta g}K_{\text{out}}^{(0)}(t)$ by taking the functional derivative with respect to the incoming dotted-line factor $(x\Omega)^{1/2}G_{\text{in}}^{(0)}(t)$, while in Eq. (3.3) we obtain $(x\Omega)^{1/2}K_{\text{in}}^{(0)}(t)$ by taking the functional derivative with respect to the outgoing dotted-line factor $(x\Omega)^{1/2}e^{\beta g}G_{\text{out}}^{(0)}(t)$. The quantities $K_{\text{out}}^{(0)}(t)$ and $K_{\text{in}}^{(0)}(t)$ will be expressed in terms of master (μ, ν) graphs in Sec. 5.

In order to make clearer the analogies between the analysis of zero-momentum self-energy structures given in this section and the analysis of nonzero-momentum self-energy structures given in Sec. 4, it is useful to express $K_{\text{out}}^{(0)}(t)$ and $K_{\text{in}}^{(0)}(t)$ in terms of zero-contracted (0, 1) and (1, 0) L graphs as

$$K_{\text{out}}^{(0)}(t) = [(x\Omega)^{1/2}e^{\beta g}]^{-1}\sum[\text{all different zero-contracted } (0,1) \ L \text{ graphs}]_{k=0} \tag{3.2'}$$

$$\text{and } K_{\text{in}}^{(0)}(t) = (x\Omega)^{1/2}\sum[\text{all different zero-contracted } (1,0) \ L \text{ graphs}]_{k=0} \ . \tag{3.3'}$$

The general definition of L graphs was given in Sec. 2.

We must now relate these zero-contracted (μ, ν) graphs to the primary linked-pair (μ, ν) graphs which were used previously to express the quantum-statistical theory. By iterating the dotted (zero-momentum) line factors in zero-contracted (μ, ν) graphs, we can verify that

$$\sum[\text{all different primary linked-pair } (\mu,\nu) \text{ graphs}] = \sum[\text{all different zero-contracted } (\mu,\nu) \text{ graphs}], \tag{3.4}$$

for $(\mu, \nu) \neq (0, 0)$. For $(\mu, \nu) \neq (0, 0)$, the external lines provide a means for differentiating between the two disconnected parts into which a primary linked-pair (μ, ν) graph can be separated by cutting one of its $k \equiv 0$ wiggly lines. Therefore, the symmetry numbers on the left-hand side of Eq. (3.4) are correctly generated by the right-hand side. For $(\mu, \nu) = (0, 0)$, there are no external lines to provide a means for differentiating between the two disconnected parts into which a primary linked-pair (0, 0) graph can be separated by cutting one of its $k \equiv 0$ wiggly lines. For this reason the zero-contracted (0, 0) graphs overgenerate the primary linked-pair (0, 0) graphs. As is proved in Sec. 5 of Ref. 3, we find

$$\sum[\text{all different primary linked-pair } (0,0) \text{ graphs}]$$

$$= \sum[\text{all different zero-contracted } (0,0) \text{ graphs}] - (x\Omega e^{\beta g})\int_0^\beta dt\, K_{\text{out}}^{(0)}(t)K_{\text{in}}^{(0)}(t) \ . \tag{3.5}$$

We can now use Eqs. (3.4) and (3.5) to express the quantum-statistical theory in terms of zero-contracted (μ, ν) graphs. From Eqs. (2.12) and (3.5), the grand potential is given by

$$\Omega f(x, \beta, g, \Omega) = (x\Omega)(e^{\beta g} - 1) - (x\Omega e^{\beta g})\int_0^\beta dt\, K_{\text{out}}^{(0)}(t)K_{\text{in}}^{(0)}(t) + \sum[\text{all different zero-contracted } (0,0) \text{ graphs}]. \tag{3.6}$$

From Eqs. (2.13) and (3.4), the momentum distribution is given by

$$\langle n(p)\rangle = \exp\{\beta[g - \omega(p)]\}\{1 + \epsilon\sum[\text{all different zero-contracted } (1,1) \text{ graphs}]_p\} \ . \tag{3.7}$$

By studying the zero-momentum self-energy structures we have taken the first step in a complete analysis of all the self-energy structures in the quantum-statistical theory. In Sec. 4 we complete the analysis by studying the nonzero-momentum self-energy structures.

4. NONZERO-MOMENTUM SELF-ENERGY STRUCTURES AND THE MOMENTUM DISTRIBUTION

In order to complete the analysis of self-energy structures that we began in Sec. 3, we now consider nonzero-momentum self-energy structures. By a nonzero-momentum self-energy structure we mean a graphical structure with two "external" lines that could connect two cluster vertices (or that could be attached to the same cluster vertex). For a quantum fluid with $\langle x\rangle \neq 0$, there are three different types of nonzero-momentum self-energy structures which we shall refer to as (1, 1), (0, 2), or (2, 0) self-energy structures. A (μ, ν) self-energy structure has μ outgoing "external" lines and ν incoming "external" lines where $\mu + \nu = 2$.

We use the momentum distribution to motivate the introduction of the quantity $\mathcal{G}_{1,1}(t_2, t_1, k)$ which represents the sum over all of the (1, 1) self-energy structures. This interpretation of $\mathcal{G}_{1,1}(t_2, t_1, k)$ suggests introducing the generalization $\mathcal{G}_{\mu,\nu}(t_2, t_1, k)$ which represents the sum over all the (μ, ν) self-energy structures. We then obtain a set of coupled integral equations for the $\mathcal{G}_{\mu,\nu}(t_2, t_1, k)$. Finally, we express the quantum-statistical theory (except for the grand potential which is treated in Sec. 5) in terms of master (μ, ν) graphs which contain three types of solid internal lines, dotted (zero-momentum) lines, external lines, and cluster vertices. The 1-vertices no longer appear. The three types of solid internal lines represent the three possible nonzero-momentum self-energy structures, and the dotted lines represent the zero-momentum self-energy structures introduced in Sec. 3. The use of master (μ, ν) graphs is analogous to the use of dressed propagators in the finite-temperature field theoretic treatment of quantum statistics.[12,30]

We begin analysis of the nonzero-momentum self-energy structures by introducing a quantity $\mathcal{G}_{1,1}(t_2, t_1, k)$ with the equation

$$\langle n(p)\rangle \equiv e^{\beta[g-\omega(p)]} \int_0^\beta dt\, \mathcal{G}_{1,1}(\beta, t, p) \ . \tag{4.1}$$

Comparison of Eqs. (3.7) and (4.1) suggests defining

$$\mathcal{G}_{1,1}(t_2, t_1, k) \equiv \delta(t_2^{(-)} - t_1) + \epsilon \mathcal{L}_{1,1}(t_2, t_1, k) \ , \tag{4.2}$$

where $$\mathcal{L}_{1,1}(t_2, t_1, k) \equiv \sum [\text{all different zero-contracted } (1,1)\ L \text{ graphs}]_k \ . \tag{4.3}$$

In Eq. (4.3), t_2 is the temperature variable assigned to the outgoing external wiggly line, and t_1 is the temperature variable assigned to the vertex to which the incoming wiggly line attaches. The rules for (μ, ν) L graphs are given at the end of Sec. 2.

Upon examining $\mathcal{G}_{1,1}(t_2, t_1, k)$, we see that it represents the sum over all (1, 1) structures that can occur between two cluster vertices. Hence, it can be referred to as the complete (1, 1) nonzero-momentum self-energy structure. In Eq. (4.2), the $\delta(t_2^{(-)} - t_1)$ term represents a single internal wiggly line (the δ function removes the dummy variable t_1 in this case), while $\mathcal{L}_{1,1}(t_2, t_1, k)$ represents all (1, 1) structures with two wiggly external lines. The $t_2^{(-)}$ in the δ function in Eq. (4.2) ensures that $t_2 > t_1$ and prevents the occurrence of wiggly-line loops [see rule (a) for primary linked-pair (μ, ν) graphs] when $\mathcal{G}_{1,1}(t_2, t_1, k)$ is used as a line factor in master (μ, ν) graphs.

The above interpretation of $\mathcal{G}_{1,1}(t_2, t_1, k)$ suggests the following generalization[33] of Eqs. (4.2) and (4.3):

$$\mathcal{G}_{\mu,\nu}(t_2, t_1, k) \equiv \delta(t_2^{(-)} - t_1)\delta_{\mu,\nu} + \epsilon \mathcal{L}_{\mu,\nu}(t_2, t_1, k) \ , \tag{4.4}$$

where $$\mathcal{L}_{\mu,\nu}(t_2, t_1, k) \equiv \sum [\text{all different zero-contracted } (\mu,\nu)\ L \text{ graphs}]_k \ , \tag{4.5}$$

for $\mu + \nu = 2$. The functions $\mathcal{G}_{0,2}(t_2, t_1, k)$ and $\mathcal{G}_{2,0}(t_2, t_1, k)$ represent the sums over the graphical structures with two incoming external lines and two outgoing external lines, respectively. In these (0, 2) and (2, 0) structures one external line has an assigned momentum label $+k$ and temperature label t_2, while the other external line has an assigned momentum label $-k$ and temperature label t_1. The function $\mathcal{G}_{0,2}(t_2, t_1, k)$ includes (0, 2) L graphs in which both incoming external lines attach to the same vertex; with such graphs we

must include a factor $\delta(t_2 - t_1)$ on the right-hand side of Eq. (4.5). We can show that

$$\mathcal{G}_{\mu,\nu}(t_2, t_1, k) = \mathcal{G}_{\mu,\nu}(t_1, t_2, -k), \quad \text{for } (\mu,\nu) = (0,2) \text{ or } (2,0) \ .$$

Integral Equations for the $\mathcal{G}_{\mu,\nu}(t_2,t_1,k)$

We begin by defining a basic graphical structure:

$$M_{\mu,\nu}(t_2, t_1, k) \equiv \sum [\text{all different proper zero-contracted } (\mu,\nu) \ L \text{ graphs}]_k \ . \tag{4.6}$$

By a *proper graph* we mean a graph which cannot be separated into two disconnected parts by cutting any *one* internal line. An improper graph is a graph which is not proper.

Now $M_{\mu,\nu}(t_2, t_1, k)$ is intended to represent all possible proper (μ,ν) structures that can occur between two cluster vertices except for a single internal wiggly line. The case of the single internal wiggly line has been allowed for in the definition of $\mathcal{G}_{\mu,\nu}(t_2, t_1, k)$ by the δ-function term in Eq. (4.4). As was also indicated for the $\mathcal{G}_{\mu,\nu}(t_2, t_1, k)$ functions, $M_{\mu,\nu}(t_2, t_1, k) = M_{\mu,\nu}(t_1, t_2, -k)$, for $(\mu,\nu) = (0,2)$ or $(2,0)$.

We next write down a simple set of integral equations relating the $\mathfrak{L}_{\mu,\nu}(t_2, t_1, k)$ and $M_{\mu,\nu}(t_2, t_1, k)$ functions

$$\begin{aligned}\mathfrak{L}_{1,1}(t_2, t_1, k) &= \int_0^\beta ds\,[\mathcal{G}_{1,1}(t_2, s, k) M_{1,1}(s, t_1, k) + \mathcal{G}_{2,0}(t_2, s, k) M_{0,2}(t_1, s, k)] \\ &= \int_0^\beta ds\,[M_{1,1}(t_2, s, k)\mathcal{G}_{1,1}(s, t_1, k) + M_{2,0}(t_2, s, k)\mathcal{G}_{0,2}(t_1, s, k)], \end{aligned} \tag{4.7}$$

$$\begin{aligned}\mathfrak{L}_{0,2}(t_2, t_1, k) &= \int_0^\beta ds\,[\mathcal{G}_{0,2}(t_2, s, k) M_{1,1}(s, t_1, -k) + \mathcal{G}_{1,1}(s, t_2, k) M_{0,2}(s, t_1, k)] - M_{0,2}^{(1)}(t_2, t_1, k) \\ &= \int_0^\beta ds\,[M_{1,1}(s, t_2, k)\mathcal{G}_{0,2}(s, t_1, k) + M_{0,2}(t_2, s, k)\,\mathcal{G}_{1,1}(s, t_1, -k)] - M_{0,2}^{(1)}(t_2, t_1, k) \ , \end{aligned} \tag{4.8}$$

$$\begin{aligned}\mathfrak{L}_{2,0}(t_2, t_1, k) &= \int_0^\beta ds\,[\mathcal{G}_{2,0}(t_2, s, k) M_{1,1}(t_1, s, -k) + \mathcal{G}_{1,1}(t_2, s, k)\, M_{2,0}(s, t_1, k)] - \delta(t_2, t_1,) M_{2,0}^{(1)}(t_2, t_1, k) \\ &= \int_0^\beta ds\,[M_{1,1}(t_2, s, k)\mathcal{G}_{2,0}(s, t_1, k) + M_{2,0}(t_2, s, k)\mathcal{G}_{1,1}(t_1, s, -k)] - \delta(t_2, t_1) M_{2,0}^{(1)}(t_2, t_1, k) \ . \end{aligned} \tag{4.9}$$

The quantities $M_{\mu,\nu}^{(1)}(t_2, t_1, k)$ are those parts of $M_{\mu,\nu}(t_2, t_1, k)$ in which both external lines attach to the same vertex within the graphs representing $M_{\mu,\nu}(t_2, t_1, k)$. The $\delta(t_2, t_1)$ is a Kronecker δ-function, and $M_{0,2}^{(1)}(t_2, t_1, k)$ is understood to contain a $\delta(t_2 - t_1)$ factor. The $M_{\mu,\nu}^{(1)}(t_2, t_1, k)$ are subtracted from $\mathfrak{L}_{\mu,\nu}(t_2, t_1, k)$ whenever both of the external lines of $\mathfrak{L}_{\mu,\nu}(t_2, t_1, k)$ attach to the *same* external vertex (see Figs. 5 and 6). This prevents the occurrence of a forbidden wiggly-line double bond [see rule (a) for primary linked-pair (μ,ν) graphs] when the $\mathcal{G}_{\mu,\nu}(t_2, t_1, k)$ are used as line factors in master (μ,ν) graphs.

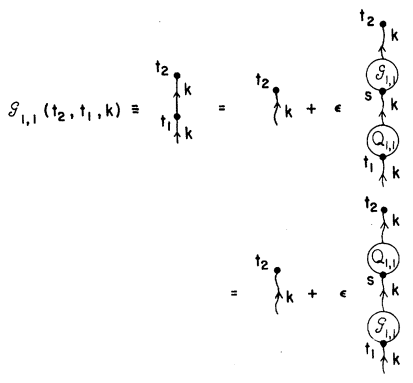

FIG. 4. Diagrammatic representation of Eqs. (4.4) and (4.13). The graphical symbol used in master (μ,ν) graphs for $\mathcal{G}_{1,1}(t_2,t_1,k)$ is also defined.

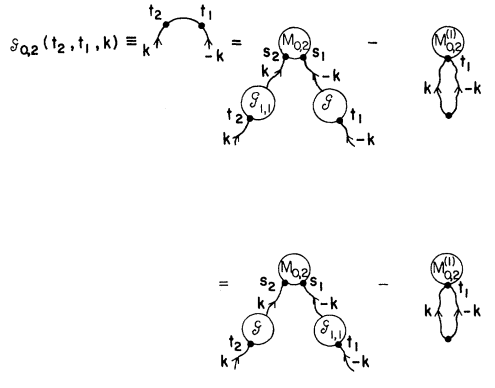

FIG. 5. Diagrammatic representation of Eqs. (4.4) and (4.14). The graphical symbol used in master (μ,ν) graphs for $\mathcal{G}_{0,2}(t_2,t_1,k)$ is also defined.

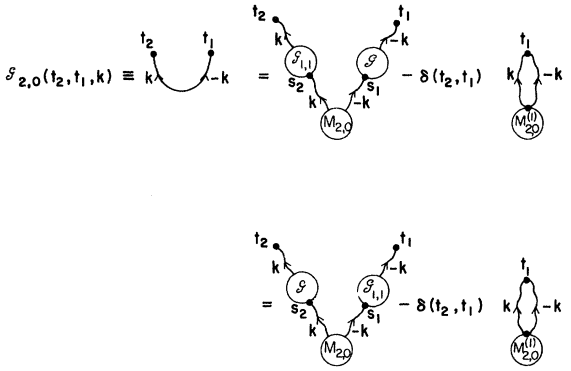

FIG. 6. Diagrammatic representation of Eqs. (4.4) and (4.15). The graphical symbol used in master (μ, ν) graphs for $\mathcal{G}_{2,0}(t_2, t_1, k)$ is also defined.

Equations (4.7)–(4.9) have the same form, but different meaning, as Eqs. (56)–(59) in Ref. 3 for $\langle x \rangle > 0$ or as Eq. (43) in Ref. 2 for $\langle x \rangle = 0$. In the same manner as we shall represent Eqs. (4.13)–(4.15) diagrammatically in Figs. 4–6, these equations can be represented diagrammatically by figures similar to Figs. 5–7 in Ref. 3, for $\langle x \rangle > 0$, and Fig. 2(a) in Ref. 2, for $\langle x \rangle = 0$. It should be remembered that for $\langle x \rangle = 0$, all (0, 2) and (2, 0) quantities are zero. Equations (4.7)–(4.9) are easily proved diagrammatically by iteration.

It is possible to obtain a partial solution to Eqs. (4.7)–(4.9) in which the integral equation for $\mathcal{G}_{1,1}(t_2, t_1, k)$ contains only a single term, and hence has the same (apparent) form for $\langle x \rangle > 0$ as it does for $\langle x \rangle = 0$ [compare Eqs. (4.7) and (4.13)]. For this purpose we introduce two new functions by the integral equation

$$\mathcal{G}(t_2, t_1, k) \equiv \delta(t_2 - t_1) + \epsilon \mathfrak{L}(t_2, t_1, k) \ , \tag{4.10}$$

$$\mathfrak{L}(t_2, t_1, k) \equiv \int_0^\beta ds \ \mathcal{G}(t_2, s, k) M_{1,1}(s, t_1, k) \ , \tag{4.11}$$

and define a function

$$Q_{1,1}(t_2, t_1, k) \equiv M_{1,1}(t_2, t_1, k) + \int_0^\beta ds_1 ds_2 M_{2,0}(t_2, s_1, k) \mathcal{G}(s_2, s_1, -k) M_{0,2}(t_1, s_2, k) \ . \tag{4.12}$$

We can consider $Q_{1,1}(t_2, t_1, k)$ as a basic (1, 1) structure in the following sense: It represents all (1, 1) structures (other than a single wiggly line) that cannot be separated into two disconnected (1, 1) structures by cutting a single internal line. Using the three functions defined by Eqs. (4.10)–(4.12), we can write a partial solution to Eqs. (4.7)–(4.9):

$$\begin{aligned} \mathfrak{L}_{1,1}(t_2, t_1, k) &= \int_0^\beta ds \, \mathcal{G}_{1,1}(t_2, s, k) Q_{1,1}(s, t_1, k) \\ &= \int_0^\beta ds \, Q_{1,1}(t_2, s, k) \mathcal{G}_{1,1}(s, t_1, k) \ , \end{aligned} \tag{4.13}$$

$$\begin{aligned} \mathfrak{L}_{0,2}(t_2, t_1, k) &= \int_0^\beta ds_1 ds_2 M_{0,2}(s_2, s_1, k) \mathcal{G}_{1,1}(s_2, t_2, k) \mathcal{G}(s_1, t_1, -k) - M_{0,2}^{(1)}(t_2, t_1, k) \\ &= \int_0^\beta ds_1 ds_2 M_{0,2}(s_2, s_1, k) \mathcal{G}(s_2, t_2, k) \mathcal{G}_{1,1}(s_1, t_1, -k) - M_{0,2}^{(1)}(t_2, t_1, k) \ , \end{aligned} \tag{4.14}$$

$$\begin{aligned} \mathfrak{L}_{2,0}(t_2, t_1, k) &= \int_0^\beta ds_1 ds_2 \, \mathcal{G}_{1,1}(t_2, s_2, k) \mathcal{G}(t_1, s_1, -k) M_{2,0}(s_2, s_1, k) - \delta(t_2, t_1) M_{2,0}^{(1)}(t_2, t_1, k) \\ &= \int_0^\beta ds_1 ds_2 \, \mathcal{G}(t_2, s_2, k) \mathcal{G}_{1,1}(t_1, s_1, -k) M_{2,0}(s_2, s_1, k) - \delta(t_2, t_1) M_{2,0}^{(1)}(t_2, t_1, k) \ . \end{aligned} \tag{4.15}$$

Equations (4.13)–(4.15) can be proved diagrammatically by iterating Eqs. (4.4) and (4.7)–(4.9) and regrouping terms. Equations (4.11)–(4.15) have the same form, but a different meaning, like Eqs. (60)–(65) in Ref. 3. The equation for $\mathfrak{L}_{1,1}(t_2, t_1, k)$ has the same form for $\langle x \rangle > 0$ as for $\langle x \rangle = 0$. Notice that when $\langle x \rangle = 0$, we have $Q_{1,1}(t_2, t_1, k) = M_{1,1}(t_2, t_1, k)$ so that $\mathcal{G}_{1,1}(t_2, t_1, k) = \mathcal{G}(t_2, t_1, k)$ and $\mathfrak{L}_{1,1}(t_2, t_1, k) = \mathfrak{L}(t_2, t_1, k)$. In Figs. 4–7, Eqs. (4.12)–(4.15) are represented diagrammatically. These diagrams are similar to those used by Beliaev[24] and by Hugenholtz and Pines.[25]

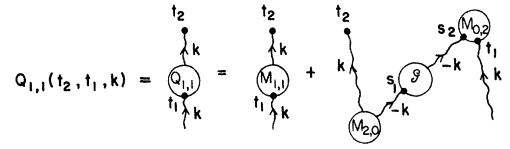

FIG. 7. Diagrammatic representation of Eq. (4.12).

Master (μ,ν) Graphs

Having completed our study of self-energy structures, we can introduce master (μ, ν) graphs and master (μ, ν) L graphs. These graphs contain cluster vertices (but no 1-vertices), three types of internal solid lines representing the three different types of nonzero-momentum self-energy structures, and dotted lines representing the zero-momentum self-energy structures. The rules for master (μ, ν) graphs are given below.

A Pth order, master (μ, ν) graph is a collection of P cluster vertices, which are entirely interconnected by m internal solid lines. There are m_{do} outgoing dotted lines and m_{di} incoming dotted lines, also referred to as internal lines. In addition to these internal solid lines, there are also μ outgoing external solid lines and ν incoming external solid lines. Each external solid line and each dotted line carries a single arrow, while each internal solid line carries two arrows, one at each end of the line. Thus, there are three different types of internal solid lines depending on whether the two arrows point parallel to each other, point towards each other, or point away from each other. At the head of each arrow carried by an internal line, there is a dot. If the arrow points towards a vertex this dot is identical with the vertex. A master (μ, ν) graph does not contain any 1 vertices. A master (μ, ν) graph is irreducible, i.e., it cannot be separated into two (or three) disconnected graphs, at least one of which is a (1, 1), (0, 2), or (2, 0) graph, by cutting any two of its internal lines. The rules for obtaining the corresponding expression for a given graph are as follows:

(a) To each external solid line assign a pregiven momentum p. External lines with different assigned momenta are distinguishable. When an external momentum is zero, there is no corresponding external line.

(b) Two master (μ, ν) graphs are different if their topological structures, including arrow directions and momentum labels of external lines (but not including the momentum labels of internal arrows and the temperature labels which will be assigned later), are different.

(c) To each arrow of the m internal solid lines assign a different integer $i(i = 1, 2, \ldots, 2m)$ and a corresponding momentum k_i. To each arrow of the $(m_{do} + m_{di})$ dotted lines assign a different integer $i(i = 2m + 1, \ldots, 2m + m_{do} + m_{di})$ and a corresponding zero momentum.

(d) Assign a factor S^{-1} to the entire graph, where

$S \equiv$ symmetry number.

The symmetry number is defined to be the total number of permutations of the $(2m + m_{do} + m_{di})$ integers assigned to the arrows of the internal lines which leave the graph topologically unchanged (including the position of these integers with respect to the arrows).

(e) Assign a different temperature variable t to each of the P vertices (circled dots) and to each of the uncircled dots (at the head end of each internal arrow that points away from a vertex). Associate with the entire graph a product of P pair functions corresponding to the P vertices with the momentum variable assignments of rules (a) and (c). The pair-function "upper temperature label" associated with an outgoing external solid line is β. Assign a factor ϵ^{P_B} to the graph, where P_B is the total permutation of the $2P$ bottom-row momenta with respect to the $2P$ top-row momenta in the product of pair functions.

(f) To each internal solid line with arrows labeled i and j assign a line factor and a momentum-conserving Kronecker δ. These assignments are: $\delta(k_i, k_j)\mathcal{G}_{1,1}(t, s, k_i)$, when the arrows point parallel to each other; $\delta(k_i, -k_j)\mathcal{G}_{0,2}(t, s, k_i)$, when the arrows point towards each other; and $\delta(k_i, -k_j)\mathcal{G}_{2,0}(t, s, k_i)$ when the arrows point away from each other, where the temperature variables t and s are determined by the assignments of rule (1). In each case the arrow labeled i points towards the dot labeled with the temperature variable t, and the arrow labeled j points towards the dot labeled with the temperature variable s.

(g) When two internal lines connect the same two vertices (with temperature variables t_3 and t_4) and have the associated line factor product $\mathcal{G}_{1,1}(t_3, t_1, k_1)\mathcal{G}_{1,1}(t_3, t_2, k_2)$, then from the quantity

$$\mathcal{G}_{1,1}(t_2, t_1, k_1)\mathcal{G}_{1,1}(t_3, t_2, k_2)^{t_1 t_2}\begin{bmatrix} k_1 & k_2 \\ k_3 & k_4 \end{bmatrix}_{t_4}$$

we must subtract the term

$$\delta(t_3-t_1)\delta(t_3-t_2)\begin{bmatrix} k_1 & k_2 \\ k_3 & k_4 \end{bmatrix}_{t_4}^{t_3 t_3} .$$

The subtracted term is called the wiggly-line double-bond correction [see rule (a) in Sec. 2].

(h) Associate with each outgoing dotted (zero-momentum) line a factor $(x\Omega)^{1/2}G_{\text{out}}^{(0)}(t)\,e^{\beta g}$, where t is the temperature variable assigned to the outgoing dotted line in rule (e). Associate with each incoming dotted line a factor $(x\Omega)^{1/2}G_{\text{in}}^{(0)}(t)$, where t is the temperature variable assigned to the vertex to which the incoming dotted line attaches.

(i) Finally, sum over the $2m$ internal momenta and integrate from 0 to β over each of the temperature variables assigned in rule (e).

We must now relate these master (μ,ν) graphs to the zero-contracted (μ,ν) graphs. By iterating the solid internal lines in master (μ,ν) graphs, we can verify that

$$\sum[\text{all different proper zero-contracted } (\mu,\nu)\ L \text{ graphs}]_k = \delta_{\mu,1}\delta_{\nu,1}\delta(\beta-t_1)\exp\beta[g-\omega(p)] + \sum[\text{all different master } (\mu,\nu)\ L \text{ graphs}]_k , \tag{4.16}$$

for $(\mu,\nu)\neq(0,0)$. The first term on the right-hand side of Eq. (4.16) represents the proper zero-contracted $(1,1)$ L graph consisting of a single 1-vertex, which is not a master $(1,1)$ L graph. It is straightforward to verify that the symmetry numbers are correctly given. It is convenient to define

$$K_{\mu,\nu}(t_2,t_1,k) \equiv \sum_{P=1} [\text{all different } P\text{th-order master } (\mu,\nu)\ L \text{ graphs}]_k , \tag{4.17}$$

so that from Eqs. (4.6) and (4.16), we obtain

$$M_{\mu,\nu}(t_2,t_1,k) = \delta_{\mu,\nu}\delta(\beta-t_1)\exp\beta[g-\omega(p)] + K_{\mu,\nu}(t_2,t_1,k) . \tag{4.18}$$

Thus, we can express the nonzero-momentum self-energy structures and the momentum distribution, Eq. (4.1), entirely in terms of master (μ,ν) L graphs.

The zero-momentum self-energy structures and the grand potential will be expressed in terms of master (μ,ν) graphs in Sec. 5.

5. MASTER-GRAPH FORMULATION OF THE GRAND POTENTIAL

The master-graph formulation outlined at the end of Sec. 4 summarizes the analysis of the self-energy problem discussed in detail in Secs. 3 and 4. The master graph line factors $\mathcal{G}_{\mu,\nu}(t_2,t_1,k)$ of Eq. (4.4) represent the sum over all possible (μ,ν) self-energy structures, where $(\mu,\nu)=(1,1)$, $(0,2)$, and $(2,0)$. By summing over all possible self-energy structures we have been able to express the zero-contracted (μ,ν) L graphs in terms of master (μ,ν) L graphs for $(\mu,\nu)\neq 0$ [See Eq. (4.16)]. In this section, we would like to express the grand potential Ωf, given by Eq. (3.6), completely in terms of master (μ,ν) graphs.

We would like to rewrite the sum over all zero-contracted (0, 0) graphs in terms of master (0, 0) graphs. To this end we define

$$\Omega f \equiv \sum[\text{all different master (0, 0) graphs}] . \tag{5.1}$$

As a first guess, one might think that ΩF equals the sum over all zero-contracted (0, 0) graphs. Unfortunately, the expansion of the right-hand side of (5.1) shows that the symmetry numbers of the zero-contracted (0, 0) graphs are not properly reproduced. Hence we must obtain an expression for the difference between ΩF and the sum over all zero-contracted (0, 0) graphs. We find that this difference can be expressed in terms of master (μ,ν) graphs by using the following quantities which are generalizations of the $\mathcal{G}_{\mu,\nu}(t_2,t_1,k)$ and $\mathcal{L}_{\mu,\nu}(t_2,t_1,k)$ defined by Eqs. (4.7)–(4.9):

$$\mathcal{G}^{(\tau)}_{\mu,\nu}(t_2,t_1,k) \equiv \delta_{\mu\nu}(t_2^{(-)}-t_1) + \epsilon\mathcal{L}^{(\tau)}_{\mu,\nu}(t_2,t_1,k) , \tag{5.2}$$

$$\mathcal{L}^{(\tau)}_{1,1}(t_2,t_1,k) = \int_0^\tau ds[\mathcal{G}^{(\tau)}_{1,1}(t_2,s,k)M_{1,1}(s,t_1,k) + \mathcal{G}^{(\tau)}_{2,0}(t_2,s,k)M_{0,2}(t_1,s,k)], \tag{5.3}$$

$$\mathfrak{L}_{0,2}^{(\tau)}(t_2,t_1,k)=\int_0^\tau ds[\mathcal{G}_{0,2}^{(\tau)}(t_2,s,k)M_{1,1}(s,t_1,-k)+\mathcal{G}_{1,1}^{(\tau)}(s,t_2,k)M_{0,2}(s,t_2,k)]-M_{0,2}^{(1)}(t_2,t_1,k)\ , \tag{5.4}$$

$$\mathfrak{L}_{2,0}^{(\tau)}(t_2,t_1k)=\int_0^\tau ds[\mathcal{G}_{2,0}^{(\tau)}(t_2,s,k)M_{1,1}(t_1,s,-k)+\mathcal{G}_{1,1}^{(\tau)}(t_2,s,k)M_{2,0}(s,t_1,k)]-\delta(t_2,t_1)M_{2,0}^{(1)}(t_2,t_1k)\ , \tag{5.5}$$

where τ is a general temperature parameter satisfying the inequality $\beta>\tau\geq(t_2,t_1)$. The functions $M_{2,0}^{(1)}(t_2,t_1,k)$ and $M_{0,2}^{(1)}(t_2,t_1,k)$ have already been defined below Eq. (4.9). The kernels of the above integral equations, namely, $M_{\mu,\nu}(t_2,t_1,k)$, are given by Eqs. (4.18).

For convenience, we have not listed the alternative expressions for $\mathfrak{L}_{\mu,\nu}^{(\tau)}(t_2,t_1,k)$, which are analogous to the second lines of Eqs. (4.7)–(4.9). It is also worth noting that the master-graph line factors $\mathcal{G}_{\mu,\nu}(t_2,t_1,k)$ are the special cases of the more general line factors $\mathcal{G}_{\mu,\nu}^{(\tau)}(t_2,t_1,k)$. Thus, it is easily verified that

$$\mathcal{G}_{\mu,\nu}^{(\beta)}(t_2,t_1,k)=\mathcal{G}_{\mu,\nu}(t_2,t_1,k)\ . \tag{5.6}$$

We will also need a partial solution to the integral equations (5.2)–(5.5) for $\mathfrak{L}_{1,1}^{(\tau)}(t_2,t_1,k)$. This solution can be written in analogy with Eqs. (4.10)–(4.13) as

$$\mathfrak{L}_{1,1}^{(\tau)}(t_2,t_1,k)=\int_0^\tau ds\,\mathcal{G}_{1,1}^{(\tau)}(t_2,s,k)\times Q_{1,1}^{(\tau)}(s,t_1,k)\ , \tag{5.7}$$

where

$$Q_{1,1}^{(\tau)}(t_2,t_1,k)\equiv M_{1,1}(t_2,t_1,k)+\int_0^\tau ds_1ds_2M_{2,0}(t_2,s_1,k)\times\mathcal{G}^{(\tau)}(s_2,s_1,-k)M_{0,2}(t_1,s_2,k), \tag{5.8}$$

$$\mathcal{G}^{(\tau)}(t_2,t_1,k)=\delta(t_2-t_1)+\epsilon\mathfrak{L}^{(\tau)}(t_2,t_1,k)\ , \tag{5.9}$$

$$\mathfrak{L}^{(\tau)}(t_2,t_1,k)=\int_0^\tau ds\,\mathcal{G}^{(\tau)}(t_2,s,k)M_{1,1}(s,t_1,k). \tag{5.10}$$

We now state the result for the difference between ΩF of Eq. (5.1) and the sum over all zero-contracted (0, 0) graphs by the following theorem:

$$\sum[\text{all different zero-contracted (0, 0) graphs}]=\Omega F+\sum_{\vec{p}}\int_0^\beta dt\,[\mathfrak{L}_{1,1}^{(t)}(t,t,p)-\mathfrak{L}_{1,1}(t,t,p)]+\sum_p\langle n(p)\rangle+\tfrac{1}{2}\sum_p\int_0^\beta dt_1\,dt_2M_{2,0}^{(1)}(t_2,t_1,k)M_{0,2}^{(1)}(t_2,t_1,k)\ . \tag{5.11}$$

Theorem (5.11) can be proved by generalizing the proof for the special case of $\langle x\rangle=0$ given in Appendix A. This generalization is outlined in Appendix B.

Substitution of Eq. (5.11) into Eq. (3.6) gives the following expression for the grand potential:

$$\Omega f(x,\beta,g,\Omega)=(x\Omega)(e^{\beta g}-1)+\Omega F^*(x,\beta,g,\Omega)+\sum_p\int_0^\beta dt\,\mathfrak{L}_{1,1}^{(t)}(t,t,p)+\tfrac{1}{2}\sum_k\int_0^\beta dt_1\,dt_2M_{2,0}^{(1)}(t_2,t_1,k)\times M_{0,2}^{(1)}(t_2,t_1,k)\ , \tag{5.12}$$

where

$$\Omega F^*(x,\beta,g,\Omega)\equiv\Omega F(x,\beta,g,\Omega)-(x\Omega)e^{\beta g}\times\int_0^\beta dt\,K_{\text{out}}^{(0)}(t)K_{\text{in}}^{(0)}(t)+\sum_p\langle n(p)\rangle-\sum_p\int_0^\beta dt\,\mathfrak{L}_{1,1}(t,t,p)\ . \tag{5.13}$$

To complete the master-graph formulation of the grand potential we still have to express the zero-momentum factors $K_{\text{out}}^{(0)}(t)$ and $K_{\text{in}}^{(0)}(t)$ in terms of master graphs. This step is easily accomplished by substituting Eq. (4.16) into the right-hand sides of Eqs. (3.2′) and (3.3′), and remembering that zero-contracted (μ,ν) L graphs are proper with respect to $k\equiv0$ lines. We obtain

$$K_{\text{out}}^{(0)}(t)=[(x\Omega)^{1/2}e^{\beta g}]^{-1}\times\sum[\text{all different master (0, 1) } L \text{ graphs}]_{k=0} \tag{5.14}$$

and $K_{\text{in}}^{(0)}(t)=(x\Omega)^{-1/2}$

$$\times\sum[\text{all different master (1, 0) } L \text{ graphs}]_{k=0}\ . \tag{5.15}$$

By comparing Eqs. (3.2′) and (3.3′) with Eqs. (3.2) and (3.3), and using the definition (5.1), we can derive the alternate expressions

$$K_{\text{out}}^{(0)}(t) = (x\Omega e^{\beta g})^{-1}[\delta(\Omega F)/\delta G_{\text{in}}^{(0)}(t)]_{\mathcal{G}} \quad (5.14')$$

and

$$K_{\text{in}}^{(0)}(t) = (x\Omega e^{\beta g})^{-1}[\delta(\Omega F)/\delta G_{\text{out}}^{(0)}(t)]_{\mathcal{G}}. \quad (5.15')$$

As indicated in Eqs. (5.14′) and (5.15′), the line factors $\mathcal{G}_{\mu,\nu}(t_2, t_1, k)$ are to be held constant in the functional differentiation.

6. SUMMARY

In this paper, we have taken the first step in the development of a useful microscopic theory of quantum fluids. As has been demonstrated in Secs. 2–5, this theory is conceptually much simpler than the earlier quantum-statistical developments of Lee and Yang[9,10] and Mohling.[1–4] Also, the analysis of the self-energy problem is approached in a more efficient manner. New and simpler diagrammatic expansions for the momentum distribution, the grand potential, and other quantities of interest have been obtained in terms of master graphs.

However, the formal expressions that we have obtained here are not yet in a useful form for application to low-temperature quantum fluids, i.e., normal Fermi and Bose fluids and degenerate Bose fluids. There are two routes for achieving this objective: the application of a Λ transformation to the present theory and the use of a generalized Hartree-Fock method in conjunction with the present theory. Both methods result in a quasiparticle description of the quantum fluids with the present theory converted into a readily usable form.

ACKNOWLEDGMENTS

The authors would like to thank the National Science Foundation for its support via grant No. GP-7696 (to FM) and a fellowship (to DWJS) during the course of this work. One of us (IRR) would like to thank the U.S. Educational Foundation in India for a travel grant and the University of Colorado for its support via a fellowship.

APPENDIX A

In this Appendix, we prove theorem (5.11) for the special case $\langle x\rangle = 0$, i.e., for a normal system. The relevant expressions for all quantities of interest for the normal system can be obtained by setting $\langle x\rangle = 0$ and hence by setting all (0, 2) and (2, 0) quantities equal to zero. With this remark Eq. (5.12), which is equivalent to theorem (5.11), can be restated for the special case $\langle x\rangle = 0$ as the following theorem to be proved in this Appendix:

$$\Omega f^{(N)}(\beta, g, \Omega) = \sum_k \int_0^\beta dt\,[\mathcal{L}^{(t)}(t, t, k) - \mathcal{L}(t, t, k)] + \sum_k \langle n(k)\rangle + \Omega F^{(N)}(\beta, g, \Omega)\ , \quad (A1)$$

where $\Omega f^{(N)}$ is the grand potential for the normal system, and $\Omega F^{(N)}$ is given by the right-hand side of Eq. (5.1) after setting $\langle x\rangle = 0$. Also $\mathcal{L}(t_2, t_1, k)$, the master-graph line factor for a normal quantum fluid [which is equal to $\mathcal{L}_{1,1}(t_2, t_1, k)$ in this case], is given by Eqs. (4.10) and (4.11) with $\langle x\rangle \equiv 0$. Similarly, $\mathcal{L}^{(\tau)}(t_2, t_1, k)$ is given by Eqs. (5.9) and (5.10) with $\langle x\rangle = 0$.

The proof of theorem (A1) involves the use of the following lemma:

$$\Omega f^{(N)}(\beta, g, \Omega) - \Omega F^{(N)}(\beta, g, \Omega) - \sum_k \langle n(k)\rangle = -\epsilon \sum_k \sum_{m=2}^{\infty} e^m \frac{m-1}{m} \int_0^\beta dt_1\, dt_2 \cdots dt_m \times M_{1,1}(t_1, t_2, k) M_{1,1}(t_2, t_3, k) \times \cdots M_{1,1}(t_{m-1}, t_m, k) \times M_{1,1}(t_m, t_1, k). \quad (A2)$$

This lemma can be proved by generalizing the proof of Eq. (54) in Ref. 2, which proof is given in Appendix B of that reference. We shall not repeat this proof here. We should note, however, that for the purposes of this proof the term $\sum_k \langle n(k)\rangle$ on the left-hand side of Eq. (A2) can be thought of as a master (0, 0) graph, constructed by closing the external line of the 1-vertex graph of Fig. 1(a) [see also Eq. (4.1)].

The right-hand side of Eq. (A2) can be rewritten in a more compact form by including the $m = 1$ term, which is zero, and then separating the m/m terms from the $1/m$ terms. We obtain

$$\Omega f^{(N)}(\beta, g, \Omega) - \Omega F^{(N)}(\beta, g, \Omega) - \sum_k \langle n(k)\rangle = -\epsilon \sum_k \sum_{m=1}^{\infty} \epsilon^m \int_0^\beta dt_1\, dt_2 \cdots dt_m \times M_{1,1}(t_1, t_2, k) \cdots M_{1,1}(t_m, t_1, k) + \epsilon \sum_k \sum_{m=1}^{\infty} \epsilon^m \int_0^\beta dt_1$$

$$\times \int_0^{t_1} dt_2 \cdots dt_m M_{1,1}(t_1, t_2, k)$$

$$\times \cdots M_{1,1}(t_m, t_1, k) \,. \tag{A3}$$

In obtaining Eq. (A3) from Eq. (A2) we have also used the following identity:

$$\frac{1}{m} \int_0^\beta dt_m \int_0^\beta dt_{m-1} \cdots \int_0^\beta dt_1 f(t_1, t_2, \ldots, t_m)$$

$$= \int_0^\beta dt_m \int_0^{t_m} dt_{m-1} \int_0^{t_m} dt_{m-2}$$

$$\times \cdots \int_0^{t_m} dt_1 f(t_1, t_2, \ldots, t_m) \,, \tag{A4}$$

which is valid whenever $f(t_1, t_2, \ldots, t_m)$ is a cyclic function of the m-temperature variables. Upon substituting the definitions (4.11) and (5.10) for the case $\langle x \rangle = 0$ into Eq. (A3), we readily derive theorem (A1).

As a final matter for this Appendix we note that the expression (A1) for the grand potential $\Omega f^{(N)}$ can also be derived by simplifying the corresponding expression for Ωf given by Eq. (56) of Ref. 2.

APPENDIX B

In this Appendix, we sketch briefly the proof of theorem (5.11). The proof involves first a generalization of theorem (A1) for the $\langle x \rangle \neq 0$ case. The first guess for such a generalization might be

$$\sum [\text{all different zero-contracted } (0,0) \text{ graphs}]$$

$$= \Omega F(x, \beta, g, \Omega) + \sum_p \langle n(p) \rangle$$

$$+ \sum_p \int_0^\beta dt \, [\mathfrak{L}_{1,1}^{(t)}(t, t, p) - \mathfrak{L}_{1,1}(t, t, p)] \,. \tag{B1}$$

This guess is almost correct. The correct generalization is obtained by adding the last term on the right-hand side of Eq. (5.11) to the right-hand side of Eq. (B1), as can be verified by following the derivation of Eq. (91) from Eq. (88) in Ref. 3. This slight modification then leads us to theorem (5.11).

An even more direct proof of theorem (5.11) involves the combined use of the proof of Eq. (88) in Ref. 3 with the analysis in Appendix G of Ref. 10. We shall not elaborate this alternate proof here.

---

*On leave of absence from Tata Institute of Fundamental Research, Colaba, Bombay-5, India.

†NRC/ESSA Postdoctoral Resident Research Associate. On leave of absence from Department of Physics, Creighton University, Omaha, Neb. 68131.

[1] F. Mohling, Phys. Rev. 122, 1044 (1961).

[2] F. Mohling, Phys. Rev. 122, 1062 (1961).

[3] F. Mohling, Phys. Rev. 135, A831 (1964).

[4] F. Mohling, Phys. Rev. 135, A855 (1964).

[5] F. Mohling, Phys. Rev. 135, A876 (1964).

[6] F. Mohling, Phys. Rev. 124, 583 (1961).

[7] F. Mohling and W. T. Grandy, Jr., J. Math. Phys. 6, 348 (1965).

[8] T. D. Lee and C. N. Yang, Phys. Rev. 113, 1165 (1959); 116, 25 (1959); 117, 12 (1960).

[9] T. D. Lee and C. N. Yang, Phys. Rev. 117, 22 (1960).

[10] T. D. Lee and C. N. Yang, Phys. Rev. 117, 897 (1960).

[11] C. De Dominicis, J. Math. Phys. 3, 983 (1962); 4, 255 (1963).

[12] C. Bloch, in Studies in Statistical Mechanics, edited by J. De Boer and G. E. Uhlenbeck (North-Holland Publishing Co., Amsterdam, 1965), Vol. III.

[13] N. N. Bogoliubov, J. Phys. (USSR) 11, 23 (1947).

[14] A. E. Glassgold, A. N. Kaufman, and K. M. Watson, Phys. Rev. 120, 660 (1964).

[15] T. D. Lee, K. Huang, and C. N. Yang, Phys. Rev. 106, 1135 (1957); T. D. Lee and C. N. Yang, *ibid.* 112, 1419 (1958).

[16] T. T. Wu, Phys. Rev. 115, 1390 (1959).

[17] K. A. Brueckner, Phys. Rev. 100, 36 (1955).

[18] J. Goldstone, Proc. Roy. Soc. (London) A239, 267 (1957).

[19] K. A. Brueckner and K. Sawada, Phys. Rev. 106, 1117 (1957).

[20] W. E. Parry and D. ter Haar, Ann. Phys. (N. Y.) 19, 496 (1962).

[21] K. Kumar, Perturbation Theory and the Nuclear Many Body Problem (North-Holland Publishing Co., Amsterdam, 1962).

[22] D. H. Kobe, J. Math. Phys. 9, 1779 (1968).

[23] P. Nozières, Theory of Interacting Fermi Systems (W. A. Benjamin, Inc., New York, 1964).

[24] S. T. Beliaev, Zh. Eksperim. i Teor. Fiz. 34, 47 (1958); 34, 433 (1958) [English transls.: Soviet Phys. – JETP 7, 289 (1958); 7, 299 (1958)].

[25] N. Hugenholtz and D. Pines, Phys. Rev. 116, 489 (1959).

[26] P. C. Martin and J. Schwinger, Phys. Rev. 115, 1342 (1959).

[27] R. D. Puff, Ann. Phys. (N. Y.) 13, 317 (1961).

[28] J. Gavoret and P. Nozières, Ann. Phys. (N. Y.) 28, 349 (1964).

[29] K. Huang and A. Klein, Ann. Phys. (N. Y.) 30, 203 (1964).

[30] P. C. Hohenberg and P. C. Martin, Ann. Phys. (N. Y.) 34, 291 (1965).

[31] A. A. Abrikosov, L. P. Gorkov, and I. E. Dzyaloshinski, Methods of Quantum Field Theory in Statistical Mechanics (Prentice-Hall, Inc., Englewood Cliffs,

N. J., 1963).

[32]The definition of untransformed pair function in Eqs. (2.10) and (2.11) differs from that used in earlier work (see Refs. 1 and 3) through the inclusion of the factor $\exp\{-t_0[\omega(k_1)+\omega(k_2)-\omega(k_3)-\omega(k_4)]\}$. We make this change so that in the following papers of this series the temperature dependence of the pair function will be more apparent [see Appendix B of F. Mohling, I. RamaRao, and D. W. J. Shea, following paper, Phys. Rev. A1, 192 (1970)].

[33]The temperature integrals of the $\mathcal{G}_{\mu,\nu}(t_2,t_1,k)$ are essentially equal to the reduced density matrices, Since $\langle n(p)\rangle = \langle p|\rho_1|p\rangle$, this equality is obvious from Eq. (4.1) for the $(\mu,\nu)=(1,1)$ case. See also Ref. 3.

PHYSICAL REVIEW A VOLUME 1, NUMBER 1 JANUARY 1970

Microscopic Theory of Quantum Fluids. II. Λ Transformation

F. Mohling
Department of Physics and Astrophysics, University of Colorado, Boulder, Colorado 80302

and

I. RamaRao *
Department of Physics, Stanford University, Stanford, California 94305

and

Dion W. J. Shea †
Aeronomy Laboratory, Environmental Science Services Administration, Boulder, Colorado 80302

(Received 4 August 1969)

In a previous paper, the master-graph formulation of the quantum-statistical theory of quantum fluids was developed. If this formulation is used to calculate the equilibrium properties of quantum fluids, apparent divergences are encountered in the low-temperature limit. In the present paper, we transform this theory by means of a Λ transformation to overcome these apparent low-temperature divergences. In this transformation, the terms in the theory which gave rise to the apparent low-temperature divergences and which represent the dominant low-temperature contributions are summed explicitly to obtain well-behaved expressions. In addition, a consistent method is developed to obtain the corrections to the dominant low-temperature contributions. Explicit expressions for the Λ-transformed theory are given for the cases of a Bose fluid above the Bose-Einstein condensation temperature and for a Fermi fluid. Finally, the physical implications of the Λ transformation are discussed.

1. INTRODUCTION

In the preceding paper, [1] we developed a quantum-statistical theory of quantum fluids and obtained the master-graph formulation of the theory through a very careful analysis of the self-energy problem. In particular, we expressed the grand potential and the momentum distribution [Eqs. (I. 5.12) and (I. 4.1)] in terms of master graphs. These quantities were functionals of five different types of line factors which arose from the self-energy analysis: the solid-line factors $\mathcal{G}_{\mu,\nu}(t_2,t_1,k)$ with $(\mu,\nu)=(1,1)$, $(0,2)$, and $(2,0)$; and the outgoing (incoming) dotted zero-momentum line factors $G_{\text{out}}^{(0)}(t)[G_{\text{in}}^{(0)}(t)]$. These line factors were expressed in terms of a set of integral equations (I. 4.4), (I. 4.10)–(I. 4.15), (I. 4.17), (I. 4.18), (I. 3.1), (I. 5.14), and (I.5.15).

The reader might expect that a simple iteration of the integral equations could be used to calculate these line factors, which iteration could, in turn, be applied to obtain meaningful expressions for the grand potential and the momentum distribution. Unfortunately, this iterative procedure cannot be used since, in the low-temperature limit, it gives apparently divergent contributions (ADC) to the line factors, and hence to the grand potential and the momentum distribution. To overcome this problem we first identify the dominant parts, which lead to ADC, of the kernels of the integral equations for the line factors and then solve the resultant approximate integral equations exactly. These